Technical University of Denmark

DTU

Sub-zero austenite to martensite transformation in a Fe-Ni-0.6wt.%C alloy

Villa, Matteo; Pantleon, Karen; Somers, Marcel A. J.

Link back to DTU Orbit

DTU Library
Technical Information Center of Denmark

Sub-zero Austenite to Martensite Transformation in a Fe-Ni-0.6wt%C alloy

Matteo Villa, Karen Pantleon, Marcel A.J. Somers

Technical University of Denmark, Department of Mechanical Engineering
DK 2800 Kgs. Lyngby, Denmark

ABSTRACT

Martensitic transformation in a model Fe-Ni-0.6wt%C alloy was investigated at sub-zero Celsius temperature. The influence of the thermal path in determining the conditions leading to the formation of martensite was studied. In the investigation, samples were austenitized and quenched, whereafter isochronal (constant cooling rate) and isothermal sub-zero Celsius treatments were applied. Magnetometry was used for describing the overall kinetics of the transformation in terms of the Johnson-Mehl-Avrami-Kolmogorov kinetics. The evolution of the transformation was also investigated with in-situ synchrotron X-ray diffraction by evaluating austenite and martensite Bragg reflections. Also, the state of internal strain in austenite was determined.

1. INTRODUCTION

Martensitic transformations in steel are usually considered athermal, i.e. the transformation is instantaneous and the degree of transformation depends only on the lowest temperature reached, not on time. This approach resulted in the Koistinen-Marburger equation[1], where the transformation is modeled as a function of temperature only, and in the erroneous practice of drawing horizontal lines for the martensite formation in TTT diagrams pointed out by Zhao and Notis[2].
Similarly, when martensite is the only product of the transformation, the morphology of martensite is usually considered to be determined by the chemical composition of the steel and the austenitization process (time, temperature and imposed plastic deformation[3,4]) only, and not on the thermal path followed during the quenching process in the M_s-M_f region.
Ansell et al.[5] were the first showing this concept to be only approximate, reporting the possibility for high cooling rates to suppress the formation of lath martensite in favor of a plate like morphology in a Fe-Ni-C alloy. The recent work of Sato et al.[6] for a Fe-Ni system confirmed that different morphologies (lath, butterfly and lenticular) can form as a function of cooling rate and the final quenching temperature. They showed that a larger fraction of austenite can be retained in the portion of material that is cooled faster and to a lower final quenching temperature due to the suppression of those emerging morphologies requiring a large plastic accommodation through the movement of dislocations.
These effects are appointed to the thermally activated nature of the martensitic transformation, first revealed by Kurdyumov and Maksimova[7], and recently demonstrated by the present authors during direct in-situ observation at sub-zero temperature,[8] and could get a relevant technological importance to design new advanced steels with improved characteristics. Nowadays, after the observation of the isothermal formation of martensite at high temperature in low carbon steel by Kim et al.[9], enforcing the rationalization by Zhao and Notis regarding the possibility for time dependency to be an intrinsic characteristic of the martensitic transformation in steel, and the exploitation of the isothermal formation of martensite in commercial alloys[10], the thermally activated nature of the martensitic transformation needs to be considered for optimization of heat treatments for steel.
In this paper the influence of the thermal cycle at sub-zero temperature on the transformation path in a Fe-Ni-C model alloy, and on the consequent buildup of stresses in the material due to transformation shape strain and interaction between martensite and retained austenite during the thermal cycle is reported and analyzed.

2. EXPERIMENTAL

2.1. Material and heat treatments

Table 1: *Thermal cycle for the sub-zero treatments. Final reheating for the sample subjected to magnetometry investigation (Vibrating Sample Magneotemtry – VSM) was performed for the purpose of baseline correction and represents the reference state for the magnetometry investigation.*

Sample VSM	Cooling 3K/min to:	Isothermal holding:	Further cooling 3K/min to:	Reheating 3K/min to:	Second cooling 3K/min to:	Final reheating 3K/min
143	143K	3h, 143K	103K	203K	103K	290K
163	163K	3h, 163K	103K	203K	103K	290K
203	203K	3h, 203K	103K	203K	103K	290K
Sample XRD	Cooling 3K/min to:	Isothermal holding:		Further cooling 3K/min to:		Reheating 3K/min
1	143K	6h, 143K		103K		290K
2	88K	4h, 88K		23K		290K

The model alloy used in the present work is an iron alloy containing 12wt% Ni and 0.6wt% C. The material was prepared by Vacuum Induction Melting as a 20 kg cast (permanent mold) from electrolytic iron, electrolytic nickel and graphite.

The as-cast material was tempered for 10h at 723K, deformed by forging to ε=-0.44 and subsequently tempered for 4h at 723K. The characteristic transformation temperatures of the material in this initial state were determined by dilatometry (DIL 805A/D) and amount to: A_1=878 K, A_3=919 K, M_s=379 K. Dilatometry was also used to determine the linear expansion coefficient of homogeneous austenite in the temperature range 573-423 K: a value of $(22.05 + 0.004 \cdot T) \cdot 10^{-6} K^{-1}$ was obtained. For investigating the martensitic transformation, the samples were austenitized at 1173 K for 30min, quenched in boiling water, quenched in ice water, and maintained at 273 K for 10 minutes. After austenitization, the samples were stored at room temperature for 1-7 days before further analysis. Thereafter the samples were subjected to different subzero treatments. The treatment conditions are reported in Table 1.

2.2. Magnetometry

Vibrating Sample Magnetometry was performed with a Lake Shore 7400 Cryotronics VSM equipped with a cryostat on cylindrical samples (Ø 3mm, 4mm height), which were mounted onto a rigid fiber pole using non-magnetic Kapton tape. A magnetic field of 1.5 T was used to bring the samples at saturation. Recording was performed every 0.5 K during the isochronal cycles and every 30 seconds during the isothermal treatment. The transformation can be followed recording the magnetic moment of the sample at saturation "*M*". The signal to noise ratio of this technique is better than 10^4, and makes it the proper choice to describe the kinetics of the transformation. As the magnetic moment is temperature dependent, the signal has to be baseline corrected for the isochronal measurements. The baseline was recorded in the reference state (see 2.1).

Magnetometry is an indirect method, as the technique itself cannot prove the formation of martensite. However, a comparative analysis of the fraction transformed between different samples can be performed assuming equivalent sample dimensions and mounting conditions in the VSM equipment (standard deviation in measured magnetization ±0.7%[11]).

2.3. X-Ray Diffraction

In-situ synchrotron X-ray diffraction, XRD, was performed at MagS station (HZB-BESSY II)[12] with a radiation of wavelength λ=0.1nm focused onto a 1mm spot, applying Bragg-Brentano geometry. Samples are 0.8 mm-thick disks with a diameter of 15 mm. The measurement conditions for f.c.c. (austenite)and b.c.t. (martensite) are collected in Table 2. Diffractograms were recorded every 16 minutes in the isothermal stage and every 9 K during isochronal treatments.

Table 2: *Measurement conditions for in-situ synchrotron X-ray diffraction investigations at λ=0.1 nm.*

	2θ range		Step size 2θ	time per step [s]	hkl (f.c.c.): γ	hkl (b.c.t.): α′
Isochronal	25°-34°	53°-62°	0.03°	0.1	111, 200, 311, 222	110/101, 220/202
Isothermal	25°-34°	38°-62°	0.02°	0.5	111, 200, 220, 311, 222	110/101, 200/002, 211/112, 220/202

The quantification of the fraction transformed during isochronal cycles was performed considering the 200_γ and 311_γ reflections of austenite and the $110/101_{\alpha'}$, $220/202_{\alpha'}$ reflections of martensite, and fitting the recorded line profiles with Lorentzian functions. The 111_γ and the 222_γ reflection of austenite where not considered due to large overlap with the more intense martensite peaks. The quantification during isothermal holding was done considering all reflections to reach best statistics and weighting only 50% of the 111_γ-$110/101_{\alpha'}$ triplet and its second order as to avoid double counting of equally oriented grains. For the reflections of martensite the intensity factor was calculated assuming the angular position of the doublets in their centroid position and summing up their multiplicity factors (cf.[13]). In the quantification procedure the atomic scattering factor was calculated from the value reported in litterature[14] by linear interpolation among the tabulated sinθ/λ values. The temperature factor was assumed to be linearly dependent on temperature and equal to 0.71 at 296 K[13]. Lattice (macro-)strains in austenite generated during the cooling and reheating cycle were evaluated in the direction parallel to the diffraction vector, comparing the change of the lattice parameter of the material with that expected due to unconstrained thermal contraction. This investigation was performed in-situ on austenite by measuring the distance between the atomic planes parallel to the sample surface averaged for the 200 and 311 reflections.

3. RESULTS AND DISCUSSION

3.1. Isochronal treatments

It is observed from Fig. 1 that different thermal cycles affect the transformation path. In the samples, the final amounts of retained austenite "RA" (see caption Fig. 1) are comparable, but the transformation paths followed differ.

Assuming that the final content of RA is similar for the samples 143, 163 and 203, the results indicate different contents of RA at the beginning of the sub-zero treatment ($RA_{203}<RA_{143}<RA_{163}$); probably due to differences in the thermal path followed during quenching. Fig. 1 shows that after storage at room temperature, austenite is stabilized, because a restart of the transformation can only proceed upon further cooling[15]. Under the reported assumption, the temperature where martensite restarts to form is the lower the higher the initial fraction of martensite is, in agreement with previous studies[16].

At the beginning of the restart, martensite forms very slowly and the process accelerates during further cooling. This indicates that the transformation involves the development of new martensite nuclei. After isothermal holding in the sub-zero Celsius range, the same stabilization effect is observed for sample 203, where the isochronal transformation was interrupted at a transformed fraction before the

bending point in the S-shaped curve (Fig.1). Clearly, a continuation of the transformation after isothermal holding at 203 K proceeds through a stage of nucleation. Similar effects, albeit to a much lesser extent, are observed for samples 163 and 143. Evidently, nucleation of martensite does occur during cooling in the entire temperature range investigated. On reheating only samples 143 and 203 show a continuation of the transformation to martensite, sample 163 has reached completion of the transformation on reaching 103 K.
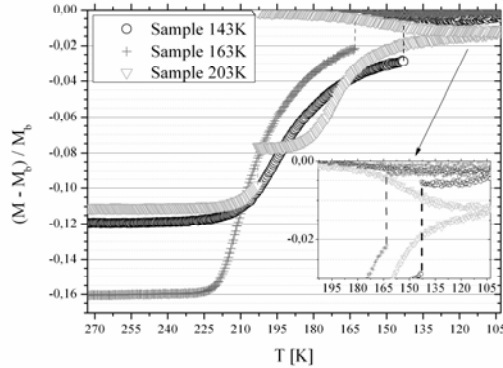

Figure 1: Baseline corrected magnetic moment at saturation, normalized to the baseline, "$(M - M_b)/M_b$" versus temperature "T" during cooling and first reheating to 203K. The discontinuities at 203K, 163K and 143K represent the isothermal part of the transformation. The magnetization at 203K during baseline recording M_b in the 2 samples was 41.43±0.02emu, indicating that comparable contents of retained austenite were obtained after the sub-zero treatment.

The effect of the thermal path on the lattice strains in austenite was investigated with XRD. Elastic straining of austenite was investigated for the thermal cycle of sample 143, albeit for an extended isothermal holding time of 6 h (SAMPLE 2). For comparison, a sample was isochronally cooled to 88 K, maintained at 88 K for 4h, further cooled to 23 K and thereafter reheated to room temperature (SAMPLE 1). The data are shown in Fig.2a, which reports the elastic strains in austenite for the two samples corrected for the thermal expansion in unconstrained conditions (taking the lattice parameter at room temperature as a reference), and in Figure 2b, which shows the fraction of retained austenite in the samples during the thermal cycle.
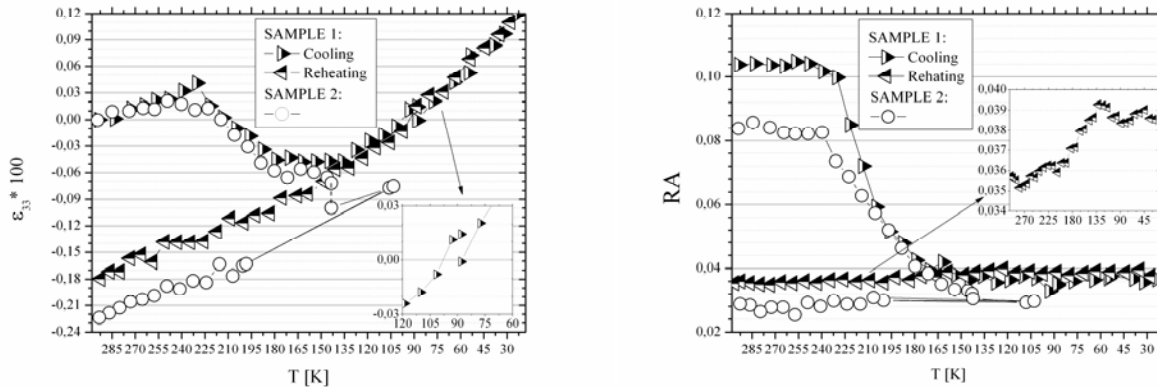

Figure 2: a) Evolution of lattice strain in austenite in the direction perpendicular to the sample surface "ε_{33}" versus temperature "T"; b) Fraction of retained austenite "RA" as a function of temperature "T". The enlarged area shows the evolution of the transformation during reheating; the data have been smoothed considering 3 points per time. For SAMPLE 2 the data in the interval region 203-103K after isothermal holding are reported only for: end of the isothermal step, first cooling to 103K, first reheating to 203K, second cooling to 103K, final reheating at 203K.

From Fig. 2 it is observed that the lattice strain is influenced by both transformation strain and interaction between phases. Since the austenite regions are very small, a state of hydrostatic strain is assumed in the following discussion of the results. During initial cooling from room temperature of the stabilized austenite, the coherency between austenite and martensite promotes a state of tension in austenite as a consequence of a larger unconstrained thermal shrink of austenite as compared to martensite, which is the majority phase in the sample.

The tension generated in austenite by constrained thermal shrink, is overcompensated by the transformation strain, because the formation of martensite in iron alloys occurs in association with a volume expansion. Consequently, when the transformation (re)starts at about 225 K (Fig. 2b), the f.c.c. lattice becomes compressed by the transformation strain, and compression increases until a temperature where the transformation rate is high enough to overcompensate the tension resulting from thermal shrink: this condition is reached at about 160 K. On continued cooling the transformation strain is visible until about 140 K, while during further cooling to 23 K only reversible elastic strain builds up (Fig.2a). This implies that only the difference in thermal shrink between austenite and martensite contributes to this strain and no irreversible volume changes associated with continued transformation or plastic deformation occur. It is noted that, since the martensite content has increased during the transformation, the strain is accommodated almost exclusively by austenite.

A very small change in compressive strain during the 4h isothermal holding at 88 K indicates that only a small amount of isothermal transformation occurs at this temperature. On reheating, the transformation restarts at about 135 K, while austenite experiences a compressive strain (Fig. 2). This temperature compares favorably with the temperature where the transformation ceased during cooling. Considering the role of straining of austenite it can be expected that compressive stress in austenite reduces the driving force for the transformation to martensite and that tension promotes this transformation. The onset of the transformation and its ceasing during cooling is consistent with this interpretation. However, the restarting of the transformation during heating, while compressive strain has built up and is further increased by continued transformation, contradicts this. Hence, the state of stress in austenite is not the only parameter determining its transformation. Most likely also a (thermally activated) mechanism is required for the transformation to be able to proceed. Regarding the overall effect of the sub-zero treatment from the technological point of view, it is important to underline that a large compressive strain in austenite at the end of the thermal cycle is observed in SAMPLE 1. Since compression stabilizes austenite[17], austenite is not only reduced, but is stabilized by the applied sub-zero treatment and reheating to room temperature.

Finally, comparing both applied thermal cycles, it is visible that isothermal holding at 143 K, allows the continuation of the transformation and a further stabilization of austenite.

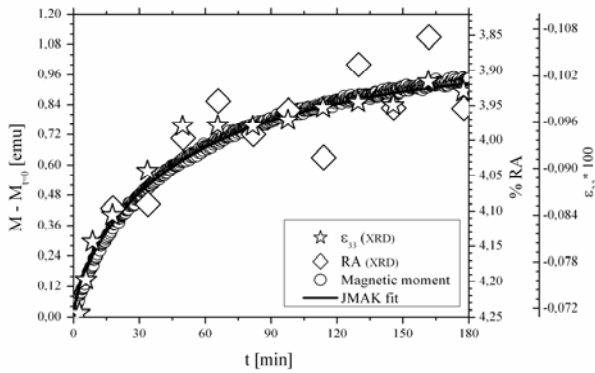### 3.2. Isothermal holding at 143K

Figure 3: Evolution of the fraction of retained austenite "RA" and of the transformation strain calculated for the 200 and 311 reflections in the direction perpendicular to the surface "ε_{33}" versus time "t" during isothermal holding. Data are compared with the increment of magnetic moment at saturation and the JMAK fit of the magnetometry results.

The evolution of the austenite-to-martensite transformation at 143 K is reported in Fig.3. This graph compares the evolution of the magnetic moment at saturation with the fraction of retained austenite and the elastic strain in austenite. The axes for austenite fraction and strain were scaled to obtain overlap with the time evolution of the magnetic moment (cf. Ref. 8). Evidently, all data recorded during the isothermal stage show similar time dependence. Qualitatively, a continuous decrease of the rate of the transformation with time implies that no nucleation of new martensite occurs in the isothermal stage, only growth of nuclei developed in the isochronal stage of the transformation. For a quantitative description of the kinetics the magnetic moment appears most appropriate, since it gives a statistical average over the entire sample, while XRD based data only apply for the information depth close to the surface of the sample.

3.3. Kinetic analysis

Kinetic analysis of the magnetometry data in the isothermal stage was performed in terms of the JMAK equation (cf. Refs. 8 and 21 for the fitting procedure). The kinetics parameter resulting from the JMAK fit, i.e. the transformation rate k and the exponent n are collected in Table 3 for the present samples as well as for data at 138 K[8]. As an example, the fit for the isothermal stage of sample143 is given in Fig.3.

T [K]	k [min]$^{-1}$	n
203	0.096	0.43
163	0.043	0.59
143	0.018	0.71
138	0.011	0.74

*Table 3: Kinetic parameters for isothermal transformation at temperature T, resulting from JMAK fit of the isothermal holding. The rate of the transformation is related to the "k" parameter, the "**n**" exponent is connected with the mechanism of phase transformation.*

Table 3 shows that the isothermal formation of martensite evolves faster at higher temperature. Moreover, the "n" exponent is the higher the lower the transformation temperature is, indicating that the transformation mechanism depends on the transformation temperature. This is consistent with previous findings and has been suggested to be related to a change of the morphology of the developing martensite[18]. In an attempt to obtain further information on the phenomenon controlling the isothermal formation of martensite, an Arrhenius dependence for "k", i.e. $k = k_0 \cdot exp\left(-\frac{E}{RT}\right)$ was assumed[19], where k_0 is a pre-exponential factor and E is the activation energy. It is noted that since the exponent n of the transformation changes with transformation temperature, strictly speaking an Arrhenius relation for k cannot be expected. Indeed, the obtained activation energy appears to increase from 7 to 17 kJ/mol with decreasing transformation temperature. The order of magnitude of the activation energy is incompatible with solid state diffusion (apart from H diffusion) of the alloying elements, which would be consistent with the characteristics of a diffusionless transformation.

4. CONCLUSIONS

Martensite formation at sub-zero temperature in a model Fe-Ni-C alloy was investigated by in-situ synchrotron XRD and magnetometry. In the isochronal stage of the transformation both nucleation and growth of martensite occurred, while only growth of pre-existing nuclei occured in the isothermal stage. After the isothermal transformation retained austenite was stabilized, implying that a restart of the transformation to martensite on continued isochronal cooling required an additional undercooling, which is consistent with the development of new martensite nuclei.

The interaction between martensite and austenite during the thermal cycle, together with the transformation strain, is important for the final stress state in the material. The difference in thermal shrink between martensite and austenite induces a tensile strain in austenite during cooling, while the transformation to martensite imposes a compressive strain onto austenite. The combination of thermal and transformation strains leads to a compressive strain in austenite after reheating to room temperature, which contributes to the stability of retained austenite.

A kinetic analysis of the austenite-to-martensite transformation in the isothermal stage indicates that the transformation mechanism depends on the sub-zero Celsius temperature and that the thermal activation involves a (diffusionless) low activation energy mechanism.

5. ACKNOWLEDGEMENT

REFERENCES

[1] D.P. Koistinen and R.E. Marburger , Acta Metall., 7 (1959) 59
[2] Ji-Cheng Zhao, Michael R. Notis, Mater. Sci. Eng., R 15 (1995) 135-207
[3] M. Umemoto and W.S. Owen, Metall. Trans., 5 (1974) 2041-2045
[4] T.N. Durlu, J. Mater. Sci., 36 (2001) 5665-5671
[5] G.S. Ansell, S.J. Donachie and R.W. Messler, JR, Metall. Trans., 2 (1971) 2443-2449
[6] H. Sato, A. Nakashima, T. Tanaka, E.M. Fujiwara, Y. Watanabe, Presented at Int. Conf. on Martensitic Transformations, Osaka, Japan, September 2011.
[7] G.V. Kurdyumov, O.P. Maksimova, Dokl Akad. Nauk SSSR 61 (1948) 83-86
[8] M. Villa, K. Pantleon, Marcel A.J. Somers, Submitted for Proc. Int. Conf. on Martensitic Transformations, Osaka, Japan, September 2011.
[9] Donghwi Kim, John G. Speer, B.C. de Cooman, Metall. Mater. Trans. A 42 (2011) 1575-1585
[10] M. Holmquist, J.O. Nilsson, A. Hultin Stigenberg, Scripta Metall. Mater., 33 (1995) 1367
[11] A. Stojko, PhD Thesis, Technical university of Denmark, Lyngby, DK, 2005
[12] E. Dudzik, R. Feyerherm, W. Diete, R. Signorato, C. Zilkens, J. Synchr. Rad. 13 (2006) 421-425
[13] ASTM International Standard designation E 975-03
[14] C.H. MacGillavry, G.D. Rieck: International Tables for X-Ray Crystallography-Vol. III physical and chemical tables, Kynoch Press
[15] O.N. Mohanty, Mater. Sci. Eng., B32 (1995) 267-278
[16] K.R. Kinsman, J.C. Shyne, Acta Metall. 15 (1967) 1527-1543
[17] J. R. Patel, M. Cohen, Acta Metall. 1:5 (1953) 531-538
[18] A. Stojko, M. F. Hansen, J. Slycke, M.A.J. Somers, J. ASTM Int. 8(4) (2011) 1-9
[19] E.J. Mittemeijer: J. Mater. Sci. Vol. 27, 1992, pp. 3977-3987